Science of the Total Environment 907 (2024) 167837

Contents lists available at ScienceDirect

Science of the Total Environment

journal homepage: www.elsevier.com/locate/scitotenv

Mechanisms of ^{137}Cs leaching based on long-term observations in forested headwater catchments in Yamakiya, Fukushima Prefecture, Japan

Taichi Kawano [a], Yuichi Onda [b,*], Hiroaki Kato [b], Junko Takahashi [b]

[a] Graduate School of Life and Environmental Sciences, University of Tsukuba, Japan
[b] Center for Research in Radiation, Isotopes and Earth System Sciences, University of Tsukuba, Japan

HIGHLIGHTS

- We explored water chemistry and seasonal ^{137}Cs changes in headwater catchments.
- In headwater stream, ^{137}Cs, DOC, and K^+ correlate positively, with no NH_4^+ detected.
- Summer boosts dissolved ^{137}Cs concentration in headwater streams 1.5–2.0x.
- The closer to the spring, the lower K^+ conc. and temperature dependence of ^{137}Cs.
- In headwater streams, dissolved ^{137}Cs vary seasonally from litter releasing ^{137}Cs.

GRAPHICAL ABSTRACT

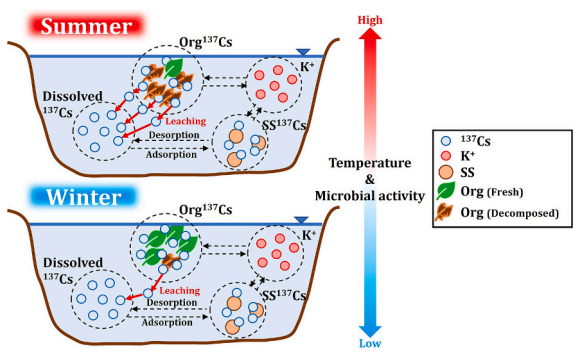

ARTICLE INFO

Editor: Jose Julio Ortega-Calvo

Keywords:
Fukushima Daiichi nuclear power plant accident
^{137}Cs
Stream water
Kd
Decontamination
Seasonal variation
DOC

ABSTRACT

Dissolved radiocesium (mainly ^{134}Cs and ^{137}Cs) is thought to be leached mainly from suspended sediment in downstream rivers, while organic matter, such as leaf litter, contributes to catchments in forested headwater streams. It is also known that dissolved ^{137}Cs in headwater streams exhibit seasonal variation with water temperature. Some mechanisms have been proposed as the causes: ionic competition of potassium ion (K^+) and ammonium ion (NH_4^+), leaching associated with the decomposition of organic matter, and thermodynamic adsorption-desorption processes. We investigated the relationship between K^+ and the dissolved organic carbon (DOC) concentrations and seasonal changes in dissolved ^{137}Cs concentration using a large number of samples from a headwater's small catchments. We examined temporal trends in ^{137}Cs concentrations in coarse organic matter, suspended sediments, and dissolved forms at four sites (one decontaminated site and three undecontaminated sites) in the Yamakiya area since 2011. The distribution coefficients (*Kdcss and Kdorg*) of dissolved ^{137}Cs concentrations relative to suspended sediment and coarse organic matter ^{137}Cs concentrations were calculated, and differences in temporal changes due to decontamination were investigated. In addition, we examined the relationship between water temperature and DOC, K^+, NH_4^+ and ^{137}Cs concentrations in the headwater catchments. The suspended sediment ^{137}Cs concentrations at the decontaminated headwater site (IBO) decreased significantly after decontamination and remained low thereafter. In contrast, dissolved ^{137}Cs concentrations decreased temporarily during the decontamination period, but returned to pre-decontamination levels. Almost no NH_4^+ has been detected in headwater streams in our catchments. In the SET and ISH watersheds, where the

* Corresponding author.
E-mail addresses: onda@geoenv.tsukuba.ac.jp, yuichionda@gmail.com (Y. Onda).

https://doi.org/10.1016/j.scitotenv.2023.167837
Received 8 April 2023; Received in revised form 12 October 2023; Accepted 12 October 2023
Available online 14 October 2023
0048-9697/© 2023 Elsevier B.V. All rights reserved.

distance from the groundwater spring is short, a correlation was found between DOC concentration and dissolved ^{137}Cs concentration. In contrast, in the IBO watershed, where the distance from the groundwater spring is long, temperature dependence and a good correlation between K^+ and ^{137}Cs were observed. Therefore, microbial decomposition of organic matter may have a significant effect on the seasonal variation of dissolved ^{137}Cs in forested headwater streams at short distances from the spring, but the influence of competing ions is expected to increase gradually as the water flows downstream.

1. Introduction

The incident at the Fukushima Daiichi Nuclear Power Plant (FDNPP) on March 11, 2011, released a large number of radionuclides into the environment and deposited 2.7 PBq of radioactive cesium-137 (^{137}Cs) on land (Onda et al., 2020). ^{137}Cs, which has a half-life of 30.1 y, may have the greatest long-term impact on human life and the surrounding ecosystem in the coming decades; therefore, enormous studies have continued to be conducted to elucidate the behavior of ^{137}Cs in the environment (e.g., Taniguchi et al., 2019; Wada et al., 2019). In the area around the Chernobyl nuclear power plant, the effects of the accident are still evident, >30 years after the incident. Various studies have been conducted since the Chornobyl accident, including field observations and model simulations of ^{137}Cs dynamics in environmental water (Smith et al., 2004). However, the topography and climatic conditions of the contaminated area around the FDNPP are very different from those around Chornobyl. First, the annual precipitation in the area surrounding the FDNPP is approximately 2.5 times higher (1105 mm) than that in the area surrounding Chornobyl (483 mm) (Konoplev et al., 2016). Second, the terrain in the area surrounding Chornobyl is flat or gently sloping, whereas the area surrounding FDNPP is mainly hilly and steep. Therefore, the ^{137}Cs migration process in the two areas cannot be directly compared, and it is important to examine the ^{137}Cs dynamics in the environment surrounding the FDNPP (Naulier et al., 2017).

Numerous studies have been conducted on the dynamics of ^{137}Cs in freshwater environments, such as the rivers and ponds in Fukushima since the FDNPP accident. Because most terrestrially deposited ^{137}Cs continue to circulate in the environment, forests located in the upper reaches of rivers are considered a potential pathway for ^{137}Cs to enter the lower reaches of rivers. ^{137}Cs discharged through rivers can be classified into three main forms: suspended sediment (SS), in which ^{137}Cs are strongly adsorbed onto fine particles; the dissolved form (Diss), in which ^{137}Cs are dissolved as ion in freshwater environments, and coarse organic matter (Org), in which ^{137}Cs is presented both outside and inside organic materials, such as litter. It has been reported that 96 % to 98 % of these three forms of the total ^{137}Cs (SS + Diss + Org) in stream waters are discharged as SS ^{137}Cs from forested catchment in the Fukushima, whereas portions of Diss (0.73 % to 3.7 %) and Org (0.92‰ to 6.9‰) forms are small in comparison compared to SS (Iwagami et al., 2017b). Therefore, it is important to clarify the interrelationships between the three phases of Diss, SS, and Org in freshwater environments to elucidate the formation mechanism of Diss ^{137}Cs concentrations.

Dissolved ^{137}Cs in headwater streams are known to exhibit seasonal variations in water temperature. Several mechanisms have been proposed as possible causes, including ion competition between potassium (K^+) and ammonium (NH_4^+) ions, leaching and adsorption inhibition associated with organic matter decomposition, and thermodynamic adsorption and desorption processes.

Regarding ionic competition, most ^{137}Cs in SS are specifically adsorbed on the frayed edge site (FES) of clay mineral particles (mainly 2:1-type layered silicates) (Sawhney, 1972) and the number of ^{137}Cs adsorption sites including FES provided by clay minerals in the environment is more than sufficient to adsorb ^{137}Cs (Delvaux et al., 2000). The FES is known to be extremely selective for Cs^+, K^+, NH_4^+ and Rb^+, and among these weakly hydrating ions, the selectivity for Cs^+ is the highest. In addition, the selectivity of the FES for Cs^+ is reported to be approximately 1000 times higher than that for K^+ and approximately 200 times higher than that for NH_4^+ (Brouwer et al., 1983; Wauters et al., 1996; McKinley et al., 2004; Nakao et al., 2008). Therefore, the higher the concentration of K^+ and NH_4^+, the more easily ^{137}Cs leaches out. Especially, some reports indicated that NH_4^+ contributed more to ion competition than K^+ in forest soil surface layers with thick O layers (Konopleva et al., 2009), lakes (Matsuzaki et al., 2021), and reservoir sediments (Funaki et al., 2022). NH_4^+ concentrations in rainfall infiltration water through the litter layer measured in the same area by co-authors Takahashi et al. (2022) ranged from 0.002 to 0.099 mmol L^{-1}. In contrast, Tsuji et al. (2016) and Tsuji et al. (2022) reported that NH_4^+ were below the detection limit (0.006 mg L^{-1}) in almost all samples from the river waters in Fukushima because NH_4^+ is quickly oxidized or absorbed by biota. Despite the importance of NH_4^+, there is still less discussion about the influence of NH_4^+ with sufficient data in headwater forested watersheds.

Regarding organic matter decomposition, ^{137}Cs and the dissolved organic carbon (DOC) have been found to leaches from organic matters. Several litter elution experiments have shown that up to 5.0 % to 33.7 % ^{137}Cs can be eluted from litter (Kurihara et al., 2020; Sakai et al., 2015; Sakakibara et al., 2021; Sakuma et al., 2021). Nakanishi et al. (2014) showed that ^{137}Cs and the dissolved organic carbon (DOC) have been found to leach from litter and soil layer by rainfall infiltration water, but these amounts from the surface soil layer were less than one-tenth of litter layers. One of the main sources of DOC is litter (Kalbitz et al., 2000), and Salamanca et al. (2003) have suggested that litter decomposition and DOC leaching are primarily controlled by microbial biological processes. In addition, temperature is the main factor determining the rate of litter decomposition (Meentemeyer, 1978). Tegen and Dorr (1996) suggested that microbial activity in forest soils with rich organic matter increased approximately twofold in response to a 10 °C increase in soil temperature and that ^{137}Cs and DOC concentrations were closely related to microbial activity. A mechanism for leaching ^{137}Cs by microbial organic matter decomposition associated with temperature changes has been proposed (Nakanishi et al., 2014); however, its impact on rivers is unclear. K^+ and DOC are more readily leached from litter than ^{137}Cs (Sakai et al., 2015). According to litter elution laboratory experiment by Kurihara et al. (2020), K^+, like ^{137}Cs, tended to elute rapidly in the early stages of Org decomposition and became less eluted as Org decomposition progressed, resulting in the elution rate of K^+ after 120 h has been reported to be approximately 10 times higher than that of ^{137}Cs. Hayashi et al. (2022) suggested that the dissolved ^{137}Cs concentration in river water was more strongly affected by indirect contribution by ionic competition of K^+ leached from the litter than direct ^{137}Cs leaching from litter under base flow conditions. However, these previous studies that observed correlations between ^{137}Cs concentrations and K^+ and DOC in watersheds (Hayashi et al., 2022; Tsuji et al., 2016; Nakanishi et al., 2021) covered a minimum of 21.0 km^2 in the upper reaches of Ota River and a maximum of 253.0 km^2 (Kido River). In relatively large watersheds such as these studies, Org originating from sources other than forests likely enters these watersheds and Diss ^{137}Cs leaching from forest-derived Org has not been accurately evaluated. Although the importance of litter has been mentioned, little research has been conducted on forest headwater catchments. Moreover, few analyses have included long-term field monitoring of ^{137}Cs. Therefore, it is necessary to report ^{137}Cs and K^+/NH_4^+ concentrations in forest headwater catchments to further investigate the dynamics of ^{137}Cs in river water.

In the field of geological disposal of radioactive wastes with temperature increase due to radioactive decay, the thermodynamic temperature dependence of adsorption equilibrium has been emphasized and various laboratory studies have been conducted (e.g., Liu et al., 2003; Tertre et al., 2005). On the other hand, Igarashi et al. (2022) showed that the adsorption entropy obtained from long-term monitoring of dissolved ^{137}Cs in a river in Fukushima was similar to the value obtained in this laboratory study, and reported that the seasonal variation of the dissolved state could be explained to some extent by thermodynamic responses. However, this is a result of a river in the lower reaches, and no study has been conducted in the upper reaches of a forested stream, which is a non-steady state that continually changes from a spring to a headwater stream.

Elucidating the leaching mechanism of Diss ^{137}Cs from forest-sourced Org is possible by conducting research in small watersheds where organic matter is abundant and there is no sediment inflow from non-forest land uses, such as agricultural land, or anthropogenic influences. Two mechanisms have been proposed for the elution of Diss ^{137}Cs from these two systems: leaching from the solid phase due to the ionic competitiveness of K^+, and leaching associated with microbial degradation of Org. Studies examining the leaching of Diss ^{137}Cs in forested headwater catchments are scarce. Long-term observations have been conducted since 2011 in the headwater catchment of the Yamakiya area (Iwagami et al., 2017a, 2017b, 2019a), and a vast amount of data have been accumulated over approximately 12.0 years. Additionally, decontamination activities have been conducted in some watersheds and it is clear that a large amount of sediment inflow has occurred (Iwagami et al., 2019a). By performing new water quality analyses of the data obtained in these studies and by analyzing a combination of Org, Diss, and SS ^{137}Cs concentrations in forested headwater catchments where organic matter is abundant, it is likely that the formation mechanism of Diss ^{137}Cs concentration in the headwater catchment can be clarified.

We observed ^{137}Cs concentrations in stream water in dissolved form, in SS, and in Org for 12.0 years after the FDNPP accident in a very small headwater basin with a watershed area of <1.0 km^2, where the contribution of leaching from forest litter dominated. Based on the long-term observation results for 12.0 years after the accident (Iwagami et al., 2017a, 2017b, 2019a), the Diss ^{137}Cs eluted from SS and Org was evaluated in terms of apparent solid-liquid distribution coefficients, and the relationship between Diss ^{137}Cs concentrations and K^+ concentrations and DOC were evaluated.

2. Materials and methods

2.1. Study site

Kawamata Town, Fukushima Prefecture is located approximately 35.0 km northwest of FDNPP and was designated as an evacuation zone after the FDNPP accident due to high ^{137}Cs contamination (0.30 MBq m^{-2} to 1.0 MBq m^{-2}; Kato et al., 2019). Four small catchments upstream of the Kuchibuto River in headwaters in the Yamakiya district of Kawamata Town (Fig. 1-a) were the subjects of this study: Iboishi-yama (IBO), Ishidaira-yama (ISH), Koutaishi-yama (KOU), and Setohachi (SET) (Fig. 1-b, Table 1). Based on the Köppen-Geiger climate classification (Peel et al., 2007), the study area can be classified as Dfa (subarctic humid climate, no dry season, hot summers) (Beck et al., 2018). According to observations between 1976 and 2022 at the Japanese Meteorological Agency's Automated Meteorological Data Acquisition System station at Nihonmatsu, the mean annual temperature is 11.8 °C and the mean annual precipitation is 1168 mm. The average temperature exceeds 20 °C in summer, and monthly precipitation reaches 200

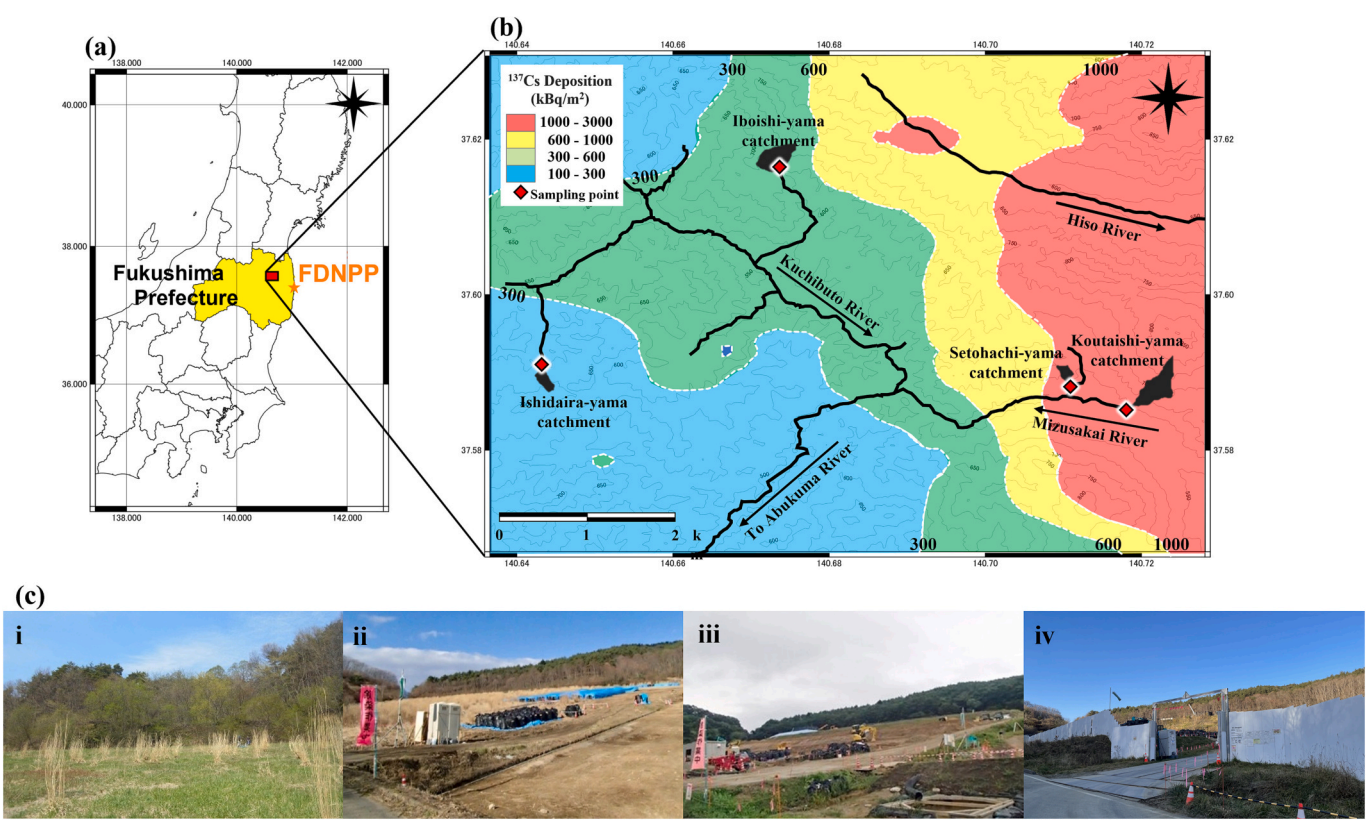

Fig. 1. Location of the study area and four small catchment observation sites.
(a) Location of the Yamakiya district, Kawamata Town, Fukushima Prefecture. (b) Location of four observation catchments in the Yamakiya district, with a color overlay of ^{137}Cs deposition. (c) Progress of decontamination at the Iboishi-yama site [i: before decontamination (10 May 2013), ii: immediately after decontamination (1 April 2014) iii: after decontamination (5 September 2014), iv: temporary storage site of decontaminated soil (23 July 2021)].

Table 1
The characteristics of observed headwater catchments and initial deposition density of ^{137}Cs.

	Catchment area (km^2)	Initial ^{137}Cs inventory (kBq m^{-2})	Number of tributaries	Maximum channel length (m)	Total channel length (m)
IBO	0.17	544	5	181.6	573.2
ISH	0.075	298	2	161.8	306.8
KOU	0.54	916	–	–	–
SET	0.048	759	2	21.9	37.0

mm in August and September, which is a major rainfall event (typhoon season), whereas the average temperature falls below 0 °C, and snowfall is observed in winter.

As shown in Table 1, the IBO site covered an area of 0.17 km^2, was composed of 23.0 % grassland and 75.6 % forest, and was centered at 37.621°N, E140.672°E. This watershed consists of five springs with a maximum channel length of 181.6 m and a total channel length of 573 m. The ISH site covers an area of 0.075 km^2, is composed of 19.0 % grassland and 81.0 % forest, and is centered at 37.597°N, 140.634°E. The KOU site covered an area of 0.54 km^2, was composed of 1.5 % grassland and 98.5 % forest, and was centered at 37.585°N, 140.709°E. This watershed consists of two springs with a maximum channel length of 161.8 m and a total channel length of 306 m. The SET site covers an area of 0.048 km^2, is composed entirely of forest, and is centered at 37.592°N, 140.709°E. This watershed consists of two springs with a maximum channel length of 21.9 m and a total channel length of 37.0 m. The initial ^{137}Cs deposition densities at the four stations were 544, 298, 916, and 759 kBq m^{-2} (Iwagami et al., 2019a, 2019b). The catchment area, initial deposition ^{137}Cs, and land use fraction for each catchment were calculated based on data from QGIS (QGIS Desktop 3.16.11, GRASS 7.8.5) and Kato et al. (2019). These small headwater catchments are located in the headwaters of the Kuchibuto and Mizusakai Rivers, which are major rivers in Fukushima Prefecture and are tributaries of the Abukuma River, a first-class river of importance for domestic and industrial use.

In Yamakiya district, approximately 98.0 % of the residents were evacuated by the end of June 2011. The area was designated as a special decontamination area, with decontamination activities beginning in March 2013 (Ministry of Environment, 2015). The entire Yamakiya District has been decontaminated since 2013. In March 2017, the evacuation of the Yamakiya district was lifted owing to a drop in the air dose rate, and some residents returned to their homes and resumed farming. In ISH, where grassland in the watershed was used as pastureland, its use resumed after the evacuation order was lifted. In the grassland area of the IBO, soil decontamination was conducted to a depth of approximately 5.0 cm, and the surface soil was removed and transplanted with uncontaminated sandy soil (Fig. 1-c). After decontamination, soil from Yamakiya District was used to fill the area, which was then used as a temporary storage site for decontaminated soil and is still being used as a temporary storage site in 2022.

2.2. Sampling and observation

Three types of sampling were collected in four small headwater catchments following the FDNPP accident. Stream water was sampled from June 2011 to December 2021. The Org and SS were sampled from August 2012 to August 2022. Sampling and observation in KOU ended in September 2013. Sampling and observation of SET began in April 2014. Stream water sampling was conducted twice monthly during 2011, at 2-month intervals during 2012–2013, at 4-month intervals during 2014, at 6-month intervals during 2015–2017, at 2- to 3-month intervals during 2018–2020, and at 1- to 2-month intervals since 2021. Org and SS sampling was conducted at 1- to 2-month intervals. Diss ^{137}Cs concentrations in stream water in ISH, IBO, SET, and KOU from June 2011 to November 2016 have been reported by Iwagami et al. (2017a, 2019a). The ^{137}Cs concentrations in Org and SS in ISH, IBO, SET, and KOU from August 2012 to November 2016 have been reported by Iwagami et al. (2017b, 2019a). In addition, the configurations of Diss and Org, SS sampling, and observation settings at each observation site were the same as those used by Iwagami et al. (2017a, 2019a).

Stream water was sampled directly from the outlet of a Parshall flume located at the observation point, and two 20.0 L polyethylene tanks (Rontainer, Collapsible One-Way Liquid Transportation Containers, SEKISUI SEIKEI CO., LTD., Osaka, Japan) of river water were collected at one time and brought back to the laboratory. Water temperature was recorded at 10.0-minute intervals using a water level gauge (TruTrack WT-HR500; Intech Instruments, Ltd., Christchurch, New Zealand) installed in a Parshall flume water-level gauge box. A time-integrated SS sampler (Phillips et al., 2000) was used to collect SS, and the collected samples were stored in 10 L polyethylene tanks (Rontainer).

Plant samples, such as leaves and branches, that entered the stream and carried the stream water was collected using 15.0 mm mesh nets placed at right angles to the flow direction. The net was placed downstream of the water level gauge, considering its effect on the stream water level if the stream channel was dammed by the accumulation of Org. Org samples were washed with stream water at the sampling points and again with tap water in the laboratory to remove the adhered sand and mud. Stream water temperature, pH, and electrical conductivity (EC) were measured at the study site using a pH/EC meter (PS-02 PH/EC; CEM Corporation, Tokyo, Japan). Stream water sampling was conducted using polyethylene containers.

2.3. Laboratory measurements

All stream water samples were stored at room temperature and filtered in the laboratory using 0.45-μm membrane filters (Advantec, Japan) within 5 days. Water samples were concentrated using the ammonium molybdophosphate (AMP)/Cs compound method (Iwagami et al., 2019a). The ^{137}Cs concentration was measured by gamma-ray spectroscopy with a germanium semiconductor detector (40 % coaxial-type Ge detector, GC4019, Canberra Industries Inc., Meriden, CT, USA). Samples with high ^{137}Cs concentrations collected immediately after the FDNPP accident were measured by the Meteorological Research Institute (Iwagami et al., 2017a).

SS and Org samples were dried in an oven at 105 °C for 24 h, crushed, and ^{137}Cs concentrations were measured using a germanium semiconductor detector (well-type GCW2022S; Canberra Industries Inc., U.S.A). After drying the SS, its particle size distribution was measured using a laser diffraction particle size analyzer (SALD-3100, Shimadzu Co., Ltd., Kyoto, Japan). Particle sizes ranged between 0.05 mm and 3.00 mm, and 51 particle size classes were defined. The particle size distributions of all SS samples were within the measured range, and all samples were attenuation-corrected on the day of collection.

Stream water samples were collected separately from the samples for Diss ^{137}Cs concentrations in polyethylene containers but filtered in the same manner as for the Diss samples. The K^+ and NH_4^+ concentrations were measured using ion chromatography (Prominence series, Shimadzu, Kyoto, Japan). The DOC concentration in the stream water was quantified using combustion catalytic oxidation (TOC-V, Shimadzu, Kyoto, Japan), and inorganic carbon was removed by acid addition before measurement.

2.4. Data analysis

2.4.1. Particle size correction of SS

^{137}Cs tend to be strongly adsorbed onto smaller particles; thus, SS with a smaller particle size and the larger specific surface area tends to have a higher ^{137}Cs concentration (He and Walling, 1996). Therefore, the particle size must be considered when evaluating the SS ^{137}Cs

concentration. Following the method described by Yoshimura et al. (2015), the SS ^{137}Cs concentration was normalized using the particle size correction factor (*P*) calculated using Eq. (1).

$$P = \left(\frac{S_r}{S_s}\right)^{v} \tag{1}$$

where S_s is the reference sample and S_r is the specific surface area (m^2 g^{-1}) assuming that the sample is spherical. The specific surface area was estimated using the particle size classification of each sample and the spherical approximation of the particles in each size category. The coefficient v was estimated for various soil and sediment samples by He and Walling (1996), who reported that v is relatively constant in the range of 0.65 to 0.75. Because v varies depending on some factors, such as the chemical composition of the particles, it is necessary to apply a value obtained under similar environmental conditions to minimize its effect. Therefore, in this study, we used $v = 0.65$ to match that reported for the Abukuma River by Yoshimura et al. (2015). Previous studies used a specific surface area of 0.202 (m^2 g^{-1}) collected on December 6, 2012, from the Mano River in Fukushima Prefecture (Yoshimura et al., 2015) as a reference sample S_s. Therefore, in this study, 0.202 (m^2 g^{-1}) was used as S_s, and the effect of particle size was corrected by dividing the ^{137}Cs concentration in the SS by *P*.

2.4.2. Radioactivity analysis

To compare multiple watersheds with different ^{137}Cs depositions, normalization was performed by dividing the ^{137}Cs concentrations (Bq L^{-1}, Bq kg^{-1}) of Diss, SS, and Org by the ^{137}Cs initial deposition (entrainment coefficient) of the watershed (Bq m^{-2}), using Eq. (2). In this case, the unit of litter (L) was converted to m^3 and the unit of normalized Diss ^{137}Cs concentration was described as m^{-1}. In addition, the particle size-corrected SS (CSS) ^{137}Cs concentration was applied to the SS ^{137}Cs concentration. This method is similar to that used to evaluate the transfer of radiocesium to plants and animals. In the evaluation of radiocesium transfer to plants and animals, the total transfer coefficient, which is the radioactivity of the biota divided by the deposition density, is often used (Rosén, 1996), whereas the entrainment coefficient is used similarly for radiocesium in the soil (Garcia-Sanchez and Konoplev, 2009; Yoshimura et al., 2015):

$$Normalized\,^{137}Cs\ concentration\left(m^{-1} or\ m^2 kg^{-1}\right) = {}^{137}Cs\ concentration\ \left(Bq\ L^{-1} or\ Bq\ kg^{-1}\right) / Average\,^{137}Cs\ deposition\left(Bq\ m^{-2}\right) \tag{2}$$

Many studies have shown that Diss ^{137}Cs concentrations in the river or stream water decrease with time after deposition. However, the reduction in Diss ^{137}Cs concentrations does not continue indefinitely, and some researchers have described the decreasing trend of Diss ^{137}Cs concentrations in stream water in the vicinity of Chornobyl after the accident using a second- or third-order exponential decay model, as shown in Eq. (3) (Smith et al., 2004). Ochiai et al. (2016) also suggest Eq. (4), which can be used when there are insufficient data to estimate the first term k_1, of Eq. (3). Eq. (4) is a first-order exponential decay model that only uses the second term in Eq. (3). Therefore, in this study, the decreasing trends in Diss, SS, and Org ^{137}Cs concentrations in stream water were estimated using Eq. (3) (Smith et al., 2002), or Eq. (4) (Ochiai et al., 2016; Nakanishi and Sakuma, 2019). Because the Diss ^{137}Cs concentrations fluctuated during rainfall, the values of the Diss ^{137}Cs concentrations sampled during rainfall were excluded from the fitting of the double exponential equation. In addition, the concentrations of samples collected at ISH on August 17, 2011, and at IBO on November 21, 2016, were excluded from the fit according to Iwagami et al. (2019a).

$$(t) = \alpha e^{k1t} + \beta e^{k2t} \tag{3}$$

$$C(t) = \beta e^{k2t} \tag{4}$$

where t is the years elapsed since the FDNPP accident, and, $C(t)$ represents the normalized Diss ^{137}Cs concentration (m^{-1}), SS ^{137}Cs concentration (m^2 kg^{-1}), and Org ^{137}Cs concentration (m^2 kg^{-1}), where each ^{137}Cs concentration (Bq L^{-1} or Bq kg^{-1}) at time t is normalized by the ^{137}Cs initial deposition (Bq m^{-2}). Monte (1997) and Smith et al. (2004) define each exponential term in Eq. (3) as follows: the first term indicates the rapid wash-off of radioactive materials seen approximately 1 a year after the accident, and the second term indicates a gradual decreasing trend due to soil fixation and redistribution that may occur approximately 2.0 to 10.0 years after the accident (Konoplev et al., 1996). In forested catchments, the apparent time scale may be extended because of the material cycling of ^{137}Cs due to litterfall from the trees (Kato et al., 2019).

2.4.3. Partition coefficients

The apparent partition coefficient (IAEA., 2020) between soil particles and organic matter (solid phase) and stream water (liquid phase) in the stream environment is expressed as the ratio between CSS and Diss ^{137}Cs concentrations and between Org and Diss ^{137}Cs concentrations, respectively (Eyrolle-Boyer et al., 2016). Therefore, in this study, the apparent solid-liquid partition coefficients of Diss ^{137}Cs concentration to CSS ^{137}Cs concentration (*Kdcss*) and Diss ^{137}Cs concentration to Org ^{137}Cs concentration (*Kdorg*) based on the long-term monitoring data of Diss, CSS, and Org ^{137}Cs concentrations are calculated using the following Eqs. (5) and (6).

$$Kd_{CSS} = \frac{C_{CSS}(t)}{C_{diss}(t)} \tag{5}$$

$$Kd_{Org} = \frac{C_{Org}(t)}{C_{diss}(t)} \tag{6}$$

where C_{diss} (Bq L^{-1}), C_{CSS} (Bq kg^{-1}), and C_{Org} (Bq kg^{-1}) are the ^{137}Cs concentrations in Diss, CSS, and Org, respectively, *at t* years after the accident. Note that this *Kd* value is the apparent partition coefficient and not the equilibrium constant of the ^{137}Cs sorption-desorption linear isotherm.

2.4.4. Seasonal variation of ^{137}Cs concentration

To investigate the seasonality of ^{137}Cs concentrations in stream water based on the long-term monitoring of ^{137}Cs concentrations, it is necessary to remove the exponential long-term decreasing trend of Diss, SS, and Org in stream water with respect to the average ^{137}Cs concentrations. Seasonality was assessed using the long-term trend removal method described by Igarashi et al. (2022). In this study, Eqs. (7), (8), and (9) were applied to the ^{137}Cs concentrations in each basin for the Diss, CSS, and Org ^{137}Cs concentrations, and the existence of the respective seasonality was examined. Org ^{137}Cs concentrations, in addition to the Diss and SS ^{137}Cs concentrations studied in the previous study, and the existence of seasonality in each was examined.

$$Diss_{det}(t) = \frac{C_{diss}(t)}{Diss_{ref}(t)} \tag{7}$$

Table 2
Parameters α, β, k_1, and k_2 for the exponential model of decreasing trends of normalized dissolved (Diss), coarse organic matter (Org) and corrected suspended sediment (CSS) ^{137}Cs concentrations, and effective half-lives (T_{eff1}, $Teff_2$).

Phase	Catchment	Sample	Parameters describing the exponential model		
First			α	k_1	T_{eff1}
			(m^{-1})	(y^{-1})	(y)
	KOU	Dissolved	2.78×10^{-2}	−14.0	0.050
	IBO	Dissolved	8.00×10^{-3}	−6.76	0.10
	ISH	Dissolved	1.92×10^{-3}	−3.12	0.22
Second			β	k_2	T_{eff2}
			(m^{-1}, $m^2\ kg^{-1}$)	(y^{-1})	(y)
	KOU	Dissolved	9.81×10^{-5}	−0.58	1.20
		Organic	1.70×10^{-3}	0.70	–
		SS	3.36×10^{-2}	−0.031	22.36
	SET	Dissolved	1.10×10^{-4}	−0.28	2.44
		Organic	1.96×10^{-2}	−0.30	2.31
		SS	5.28×10^{-2}	−0.14	4.95
	IBO	Dissolved	9.74×10^{-5}	−0.23	3.01
		Organic	1.84×10^{-2}	−0.46	1.50
		SS(Before decontamination work)	3.97×10^{-2}	−0.16	4.42
		SS(Decontamination work)	3.16×10^{5}	−5.55	0.12
		SS(After decontamination work)	1.36×10^{-3}	−0.006	115.54
	ISH	Dissolved	2.87×10^{-4}	−0.34	2.04
		Organic	1.06×10^{-2}	−0.33	2.11
		SS	4.93×10^{-2}	−0.245	2.83

$$SS_{det}(t) = \frac{C_{CSS}(t)}{SS_{ref}(t)} \tag{8}$$

$$Org_{det}(t) = \frac{C_{Org}(t)}{Org_{ref}(t)} \tag{9}$$

where $Diss_{det}$ (t), SS_{det} (t), and Org_{det} (t) are the trend-removed Diss, CSS, and Org ^{137}Cs concentrations *in t* years calculated after the accident, respectively. $Diss_{re}(t)$ (Bq L^{-1}), $SS_{ref}(t)$ (Bq kg^{-1}), and $Org_{ref}(t)$ (Bq kg^{-1}) are the Diss, CSS and Org ^{137}Cs concentration at t years estimated from the Eqs. (3) or (4) in each catchment (Table 2).

2.5. Statistics analysis

Statistical analysis for the exponential fitting of ^{137}Cs concentrations and their approximate parameters was performed using MS Excel based on the log-transformed data. The concentration of ^{137}Cs in the environment fluctuates because of various natural environmental factors such as seasonal variations, rainfall, water temperature, and flow rate, the intensity of which may be influenced by factors that have a major impact on the watershed environment, such as typhoons. Therefore, outliers in ^{137}Cs concentrations were determined using the interquartile range (IQR) in this study. Values less than (Q1–1.5 × IQR) and larger than (Q3 + 1.5 × IQR) were defined as outliers. The Tukey–Kramer multiple comparison test was used to assess the significance ($p < 0.05$) of ^{137}Cs concentrations in each group.

3. Results

3.1. Diss, Org, and CSS ^{137}Cs concentrations after the FDNPP accident

The ^{137}Cs concentrations in Diss, CSS, and Org were normalized by the initial ^{137}Cs deposition in each catchment using Eq. (2), and a reference sample with a specific surface area of 0.202 $m^2\ g^{-1}$ is shown in Fig. 2-a, -b, and -c, respectively.

The normalized ^{137}Cs concentrations of Diss, SS, and Org decreased over time in all catchments. Values between June 2011 October 2013 and November 2016 ($t = 2.5$ to 6.0 y) were based on the data reported by Iwagami et al. (2019a). For $t \leq 6.0$ y, the normalized Diss ^{137}Cs concentrations of IBO, ISH, and SET showed concentrations of the order of 10^{-5} m^{-1}. The normalized Diss ^{137}Cs concentrations at IBO, ISH, and SET were on the order of 10^{-6} to 10^{-3} m^{-1} until $t \approx 12.0$ y. In particular, the normalized Diss ^{137}Cs concentrations in SET showed a significant increase from 10^{-6} to 10^{-5} m^{-1} after Typhoon *Hagibis* or Typhoon No. 19 ($t \approx 8.6$ y, October 2019). The normalized Diss ^{137}Cs concentrations and the associated decline parameters (α, β, k_1, k_2) and T_{eff1} and T_{eff2} for the four watersheds are shown in Table 2.

The normalized CSS ^{137}Cs concentrations at IBO, ISH, SET, and KOU were of the order of 10^{-3} to 10^{-2} $m^2\ kg^{-1}$ before decontamination and of the order of 10^{-4} to 10^{-2} $m^2\ kg^{-1}$ after decontamination. Because the normalized CSS ^{137}Cs concentrations at IBO showed a sharp decrease of approximately one order of magnitude due to decontamination activities, three periods: before, during, and after restoration were compared. Immediately after the decrease in the normalized CSS ^{137}Cs concentration, the values at IBO were of the order of 10^{-4} $m^2\ kg^{-1}$, and the minimum and maximum values of IBO during the decontamination period were 3.16×10^{-4} $m^2\ kg^{-1}$ (October 6, 2014) and 5.56×10^{-2} $m^2\ kg^{-1}$ (October 25, 2013), respectively. In contrast, the minimum and maximum values at the IBO after decontamination were 1.13×10^{-4} $m^2\ kg^{-1}$ (July 11, 2019) and 4.78×10^{-3} $m^2\ kg^{-1}$ (November 16, 2017), respectively. A similar decrease in normalized CSS ^{137}Cs concentrations by approximately one order of magnitude due to decontamination was reported by Taniguchi et al. (2019) at the upstream Mizusakai site on the Kuchibuto River, which is downstream of the IBO. Normalized CSS ^{137}Cs concentrations at SET were higher than those at IBO and ISH throughout the study period; however, they were temporarily lowered by approximately one order of magnitude to the order of 10^{-3} $m^2\ kg^{-1}$ because of the effect of Typhoon *Hagibis*. However, unlike the normalized Diss ^{137}Cs concentrations, the normalized CSS ^{137}Cs concentrations did not continuously show low values after the typhoon but tended to recover to the order of 10^{-2} $m^2\ kg^{-1}$ within six months.

The normalized CSS ^{137}Cs concentrations in these four catchments can be expressed by an exponential model, The k_2 values of the normalized CSS ^{137}Cs concentrations at ISH and SET gradually increase and decrease at a slower rate during the period $t = 3.0$ to 12.0 y. The k_2 value of the normalized CSS ^{137}Cs concentration after IBO decontamination increased slightly for $t = 12.0$ y compared to $t = 6.0$ y, and the decreasing trend of the normalized CSS ^{137}Cs concentration slowed compared to that immediately after decontamination. The Org samples collected in this study mainly consisted of hardwoods and grasses, with little or no conifer contamination at all sampling sites. The ^{137}Cs concentrations in coarse organic matter and forest litter are comparable (Iwagami et al., 2019a). The normalized Org ^{137}Cs concentrations can be expressed by the first-order exponential model in all three basins, except

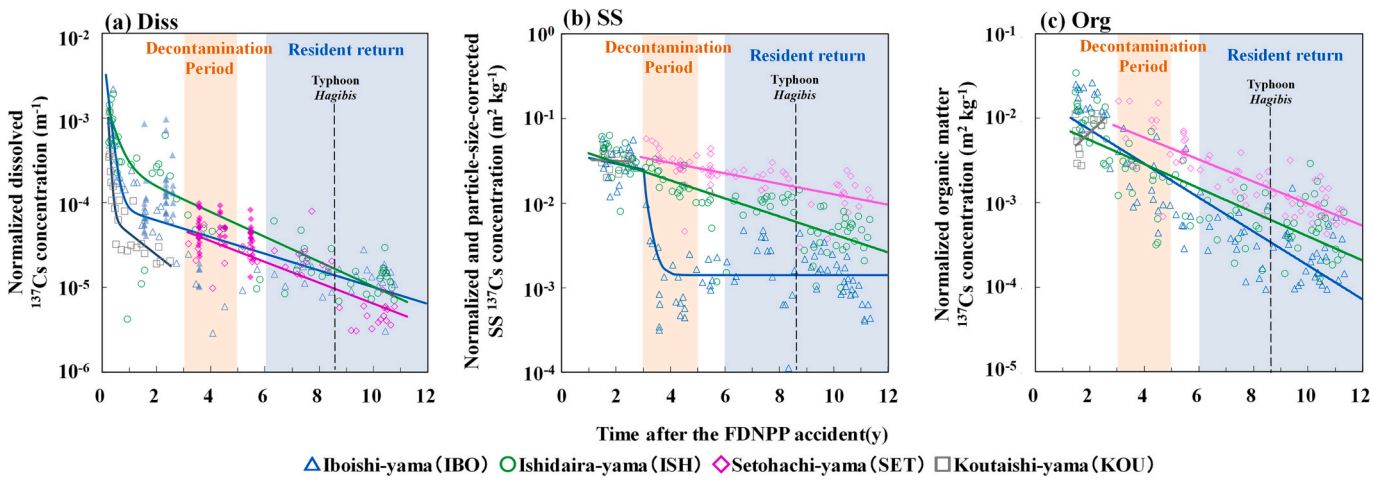

Fig. 2. Time series for 12.0 y of normalized ^{137}Cs concentrations in (a) dissolved form (Diss) (b) suspended sediment (SS), and (c) coarse organic matter (Org), for the four catchments (Iboishi-yama (IBO), Ishidaira-yama (ISH), Setohachi (SET), and Koutaishi-yama (KOU), and their fitted exponential relationships. In this figure, the filled points represent the normalized ^{137}Cs concentrations during rainfall, and each solid line represents an exponential approximation curve excluding the normalized ^{137}Cs concentrations during rainfall. The normalized SS ^{137}Cs concentration in this graph represents the normalized corrected-SS ^{137}Cs concentration with the reference sample of 0.202 (m^2 g^{-1}). The orange shading indicates the decontamination period at IBO, and the blue shading indicates the period after the evacuation order was lifted and the return of residents in the Yamakiya district.

KOU (see Table 2).

The Diss and CSS ^{137}Cs concentrations at SET were affected by Typhoon *Hagibis*, but no clear typhoon effect was observed on Org ^{137}Cs concentrations, suggesting that the source of the organic material was the same as before. The normalized Org ^{137}Cs concentrations showed an exponentially decreasing trend, except for KOU: $k_2 = -0.46$ y^{-1}, -0.33 y^{-1}, -0.30 y^{-1}, and 0.70 y^{-1} at IBO, ISH, SET, and KOU, respectively. The increasing trend at KOU was attributed to the low concentration of Org ^{137}Cs from September to November 2012 (Iwagami et al., 2019a), suggesting that large quantities of uncontaminated Org may have been present. In comparison, we cited results of Iwagami et al., 2017b and 2019b; $k_2 = -0.92$ y^{-1} for $t = 2.5$ y at ISH (Iwagami et al., 2017b), and at $t = 6.0$ y $k_2 = -0.85$ y^{-1}, -0.68 y^{-1}, -0.33 y^{-1}, and 0.701 y^{-1} for IBO, ISH, SET, and KOU, respectively (Iwagami et al., 2019a). At SET, k_2 did not change significantly during the period from t = 6.0 and 12.0 y; whereas for IBO and ISH, k_2 increased with time.

3.2. Solid-liquid distribution coefficient (Kdcss and Kdorg) of corrected-SS and organic matter

Fig. 3 shows that at IBO, the only decontaminated site, *Kdcss*, and *Kdorg*, have significant decreasing trends, with slopes of -0.121 y^{-1} and -0.302 y^{-1}, respectively. No significant trends were observed for *Kdcss* or *Kdorg* in ISH, an undecontaminated site, with slopes of 0.124 y^{-1} and 0.050 y^{-1}, respectively. However, a significant increasing trend with a slope of 0.238 y^{-1} was observed for *Kdcss* at SET, whereas no significant trend was observed for *Kdorg*, with a small slope of 0.0706 y^{-1}.

Kdcss was on the order of 10^4 to 10^6 L kg^{-1} in all watersheds until March 2013, before decontamination. After March 2013, *Kdss* continuously showed an order of 10^4 to 10^6 L kg^{-1} in the undecontaminated areas of ISH and SET, whereas those in the decontaminated area of IBO showed an order of 10^3 to 10^5 L kg^{-1} after decontamination. During the post-decontamination period, the range of values in the decontaminated area was one order of magnitude lower than that of the

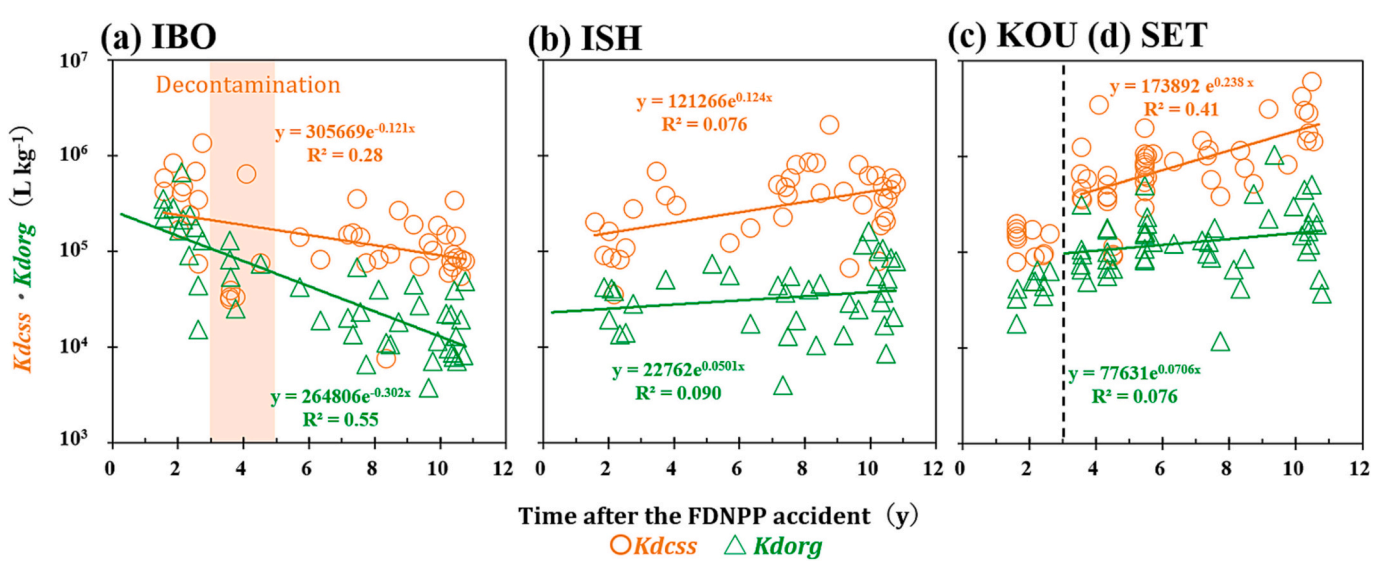

Fig. 3. Changes over time in the apparent solid-liquid partition coefficient of Diss ^{137}Cs concentration with respect to CSS-^{137}Cs concentration (○ *Kdcss*) and the apparent solid-liquid partition coefficient of Diss ^{137}Cs concentration with respect to Org ^{137}Cs concentration (△ *Kdorg*) in the four source small catchments (a: IBO, b: ISH, c: KOU d: SET).

undecontaminated area.

Before decontamination (until March 2013), the minimum values of *Kdcss* in the IBO, ISH, and KOU catchments were 7.43 × 10^4 L kg^{-1} (October 15, 2013),3.56 × 10^4 L kg^{-1} (May 11, 2013), and 6.39 × 10^5 L kg^{-1} (October 1, 2012), respectively, whereas the maximum values were 1.35 × 10^6 L kg^{-1} (December 9, 2013), 2.02 × 10^5 L kg^{-1} (October 9, 2012), and 2.60 × 10^6 L kg^{-1} (October 1, 2012), respectively. During the decontamination period (March 2013 to March 2016) the minimum values of *Kdcss* in the IBO, ISH, SET, and KOU catchments were 3.13 × 10^4 L kg^{-1} (October 6, 2014), 3.56 × 10^4 L kg^{-1} (May 11, 2013), 8.93 × 10^4 L kg^{-1} (September 18, 2015) and 7.68 × 10^5 L kg^{-1} (April 17, 2013), respectively, whereas the maximum values were 1.35 × 10^6 L kg^{-1} (December 9, 2013), 6.80 × 10^5 L kg^{-1} (October 26, 2014), 3.43 × 10^6 L kg^{-1} (April 9, 2015), 1.17 × 10^8 L kg^{-1} (March 18, 2013) respectively. After decontamination (after March 2016), the minimum values of *Kdcss* in the IBO, ISH, and SET catchments were 7.53 × 10^3 L kg^{-1} (July 12, 2019), 6.76 × 10^4 L kg^{-1} (July 18, 2020), and 2.91 × 10^5 L kg^{-1} (August 22, 2016), respectively, whereas the maximum values were 3.55 × 10^5 L kg^{-1} (August 28, 2018), 2.08 × 10^6 L kg^{-1} (December 5, 2019) and 5.99 × 10^6 L kg^{-1} (August 27, 2021).

Before decontamination (until March 2013), the minimum values of *Kdorg in* the IBO, ISH, and KOU catchments were 1.64 × 10^5 L kg^{-1} (April 9, 2015), 4.93 × 10^4 L kg^{-1} (March 18, 2013), and 6.83 × 10^4 L kg^{-1} (October 1, 2012), respectively, and the maximum values were 3.57 × 10^5 L kg^{-1} (September 30, 2012), 4.23 × 10^4 L kg^{-1} (January 17, 2013), and 3.21 × 10^5 L kg^{-1} (March 18, 2013), respectively. For the decontamination period (March 2013–March 2016), the maximum *Kdorg* values in the IBO, ISH, SET, and KOU watersheds were 4.04 × 10^4 L kg^{-1} (December 10, 2014), 8.82 × 10^4 L kg^{-1} (July 16, 2013), 8.19 × 10^4 L kg^{-1} (September 18, 2015), 8.58 × 10^5 L kg^{-1} (April 17, 2013), respectively, and the maximum values were 6.64 × 10^5 L kg^{-1} (April 17, 2013), 4.10 × 10^6 L kg^{-1} (December 9, 2014), 3.14 × 10^6 L kg^{-1} (April 9, 2015), 2.03 × 10^6 L kg^{-1} (September 19, 2013), respectively. After decontamination (after March 2016), the minimum values of *Kdorg in* the IBO, ISH, and SET catchments were 3.76 × 10^3 L kg^{-1} (October 30, 2020), 4.03 × 10^3 L kg^{-1} (July 10, 2018), and 1.18 × 10^4 L kg^{-1} (November 30, 2018), respectively, and the maximum values were 6.92 × 10^4 L kg^{-1} (August 28, 2018), 9.43 × 10^4 L kg^{-1} (June 10, 2021), and 1.04 × 10^6 L kg^{-1} (July 18, 2020).

Until March 2013, the *Kdorg* in the decontaminated area of IBO was on the order of 10^5 L kg^{-1}, 10^4 to 10^5 L kg^{-1} during decontamination, and 10^3 to 10^4 L kg^{-1} after decontamination, showing clear differences by period. In contrast, *Kdorg* in the un-decontaminated areas of ISH and SET was continuously on the order of 10^4 to 10^5 L kg^{-1}.

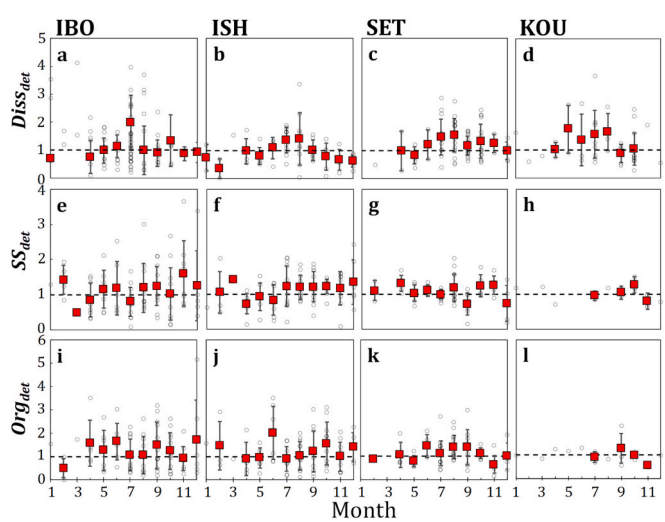

Fig. 4. Monthly changes in detrended Diss, CSS, and Org ^{137}Cs concentrations in four stream headwater small catchments (IBO, ISH, SET, and KOU) over the 12.0 years. Circles (○) indicate detrended Diss, CSS, and Org ^{137}Cs concentrations. Red squares (■) indicate the monthly means of detrended Diss, CSS, and Org ^{137}Cs concentrations, and error bars indicate standard deviation.

3.3. Seasonality of Diss, SS, and Org ^{137}Cs concentrations

The seasonal trend of ^{137}Cs concentration was evaluated using the trend removal Eqs. (7)–(9) proposed by Igarashi et al. (2022) to identify the seasonal trend of ^{137}Cs concentration, which showed an exponentially decreasing trend with time. The results for the four small headwater catchments IBO, ISH, SET, and KOU for $Diss_{det}$, SS_{det}, and Org_{det}, where the temporal decreases in dissolved ^{137}Cs, CSS ^{137}Cs, and Org ^{137}Cs concentrations were removed using Eqs. (7)–(9) are shown in Fig. 4.

The highest values of $Diss_{det}$ for IBO, ISH, and SET were 1.98 ± 0.99 (July), 1.63 ± 0.95 (July), and 1.65 ± 0.59 (August), respectively, and the lowest were 0.70 ± 0.087 (January), 0.36 ± 0.34 (February) and 0.99 ± 0.70 (April), respectively. A clear seasonal trend was observed for $Diss_{det}$ in the three basins, IBO, ISH, and SET, with maxima in July or August, a decrease from September, minima between November and February, and an increase from March (Fig. 4-a, -b, and -c). These seasonal variations showed a tendency for Diss ^{137}Cs concentrations to be up to 1.5 to 2.0 times higher than the reference values during the summer months. No clear seasonal trend was observed at KOU, which may be attributed to the short observation period and the fact that most of the observations were acquired during summer.

Although no statistically significant differences were found in $Diss_{det}$ in the headwaters, comparisons by season, spring (March–May), summer (Jun–August), fall (September–November), and winter (December–February), revealed significant differences. At IBO, $Diss_{det}$ was significantly higher in summer (1.65 ± 1.02) than in fall (1.08 ± 0.66) ($p < 0.05$) and winter (0.87 ± 0.33) ($p < 0.05$), but there was no significant difference between summer (1.65 ± 1.02) and spring (0.96 ± 0.52) ($p = 0.051$). Additionally, no significant differences were found in IBO for combinations other than summer (spring–fall, $p = 0.96$; spring–winter, $p = 0.99$; fall–winter, $p = 0.89$). At ISH, $Diss_{det}$ in summer (1.25 ± 0.54) was also significantly higher than in fall (0.84 ± 0.44) ($p < 0.05$) and winter (0.60 ± 0.33) ($p < 0.01$), but no significant difference was observed between summer (1.25 ± 0.54) and spring (0.935 ± 0.41) ($p = 0.18$). No significant differences were found in ISH for combinations other than summer (spring–fall: $p = 0.96$; spring–winter: $p = 0.56$; autumn–winter: $p = 0.80$). Conversely, at SET, $Diss_{det}$ was significantly higher in summer (1.56 ± 0.69) than in spring (0.85 ± 0.46) ($p < 0.05$) and winter (0.80 ± 0.26) ($p < 0.01$), whereas no significant difference was found between summer (1.56 ± 0.69) and fall (1.25 ± 0.49) ($p = 0.10$). No significant differences were found in SET for combinations other than summer (Table 3).

3.4. Relationship between Diss ^{137}Cs, K^+, and DOC

Because the detrended Diss ^{137}Cs concentrations *of* SS_{det} and Org_{det} did not show clear seasonal variations, factors other than CSS and Org ^{137}Cs concentrations were considered to control the seasonality of $Diss_{det}$. The NH_4^+concentrations in stream water measured in 2021–2022

Table 3
Detrended Diss ($Diss_{Det}$) in four small headwater catchments Multiple comparison tests of ^{137}Cs concentrations between seasons.

	Spring	Summer	Autumn	Winter
IBO	0.96 ± 0.52^a	1.65 ± 1.02^b	1.08 ± 0.66^{ab}	0.87 ± 0.33^b
ISH	0.94 ± 0.41^a	1.25 ± 0.54^{ab}	0.84 ± 0.44^b	0.60 ± 0.33^b
KOU	–	–	–	–
SET	0.85 ± 0.46^a	1.56 ± 0.69^{ab}	1.25 ± 0.49^b	0.80 ± 0.26^b

Superscripts a and b indicate significant differences between seasons ($p < 0.05$, Tukey's test).

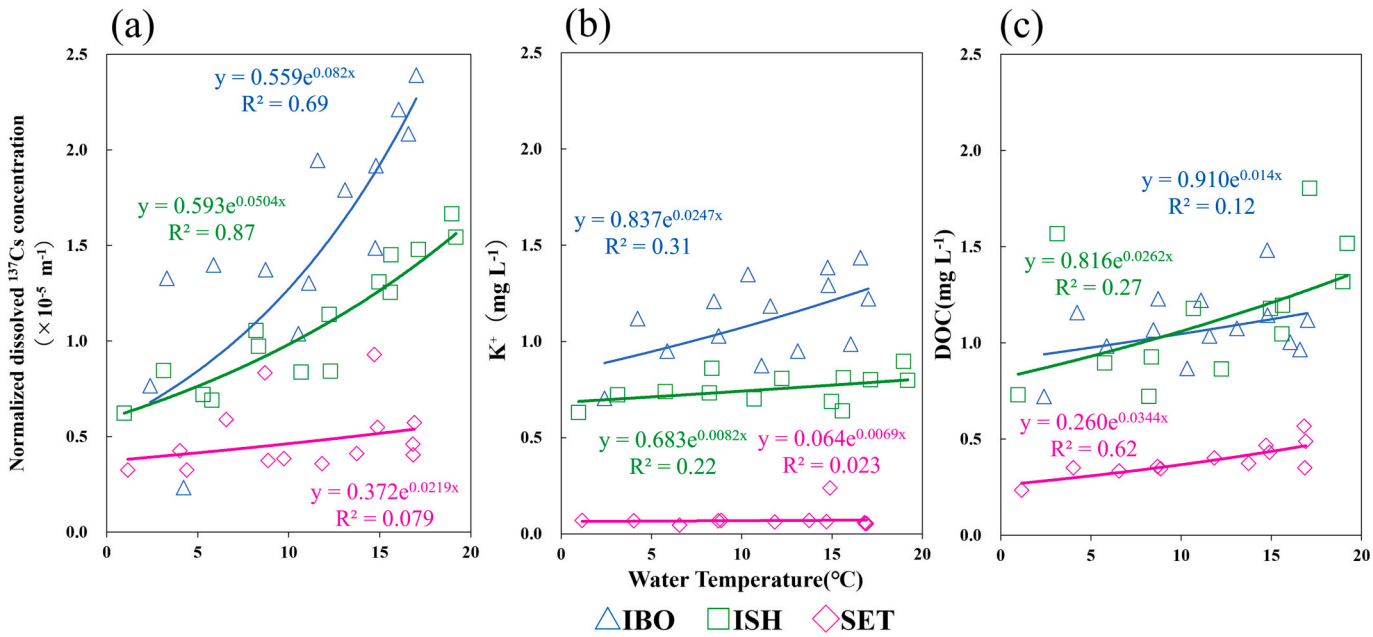

Fig. 5. Relationship between Diss ^{137}Cs concentration and (a) K^+, (b) DOC concentrations, and (c) water temperature in three catchments. The water temperature on the horizontal axis represents the average water temperature over the 10 days preceding the sampling date.

were always below the detection limit (0.001 mol L^{-1}) in ISH and at a maximum of approximately 0.007 mmol L^{-1} in SET and IBO; thus, we cannot correlate with NH_4^+ and ^{137}Cs concentrations. Tsuji et al. (2016) also state that NH_4^+ in river water are almost below the detection limit. Therefore, the relationship between K^+, DOC, and Diss ^{137}Cs concentrations and water temperature in the IBO, ISH, and SET catchments was investigated for 2021 to 2022.

The relationships between K^+, DOC, and normalized Diss ^{137}Cs concentrations and water temperature in the IBO, ISH, and SET catchments are shown in Fig. 5. The normalization of ^{137}Cs concentration was affected by decontamination for IBO. Therefore, a ^{137}Cs removal rate of 78 % (Takahashi, Personal com) due to slope decontamination was used as a reference and then multiplied by the decontamination area to obtain a new average deposition in the watershed. Significant positive correlations between the normalized Diss ^{137}Cs concentration and water temperature were observed for IBO ($R^2 = 0.69$, $p < 0.001$) and ISH ($R^2 = 0.87$, $p < 0.001$) by exponential fitting (Nakanishi and Sakuma, 2019); however, no significant relationship was found for SET. The exponent is 0.082 for IBO, 0.05 for ISH, and 0.02 for SET, indicating that the temperature dependence of Cs concentration becomes more pronounced as the length of the tributary increases. This suggests that leaching during the downstream process from the spring may be important.

A significant positive correlation between K^+ concentrations and water temperature were found for IBO ($R^2 = 0.31$, $p = 0.039$); however,

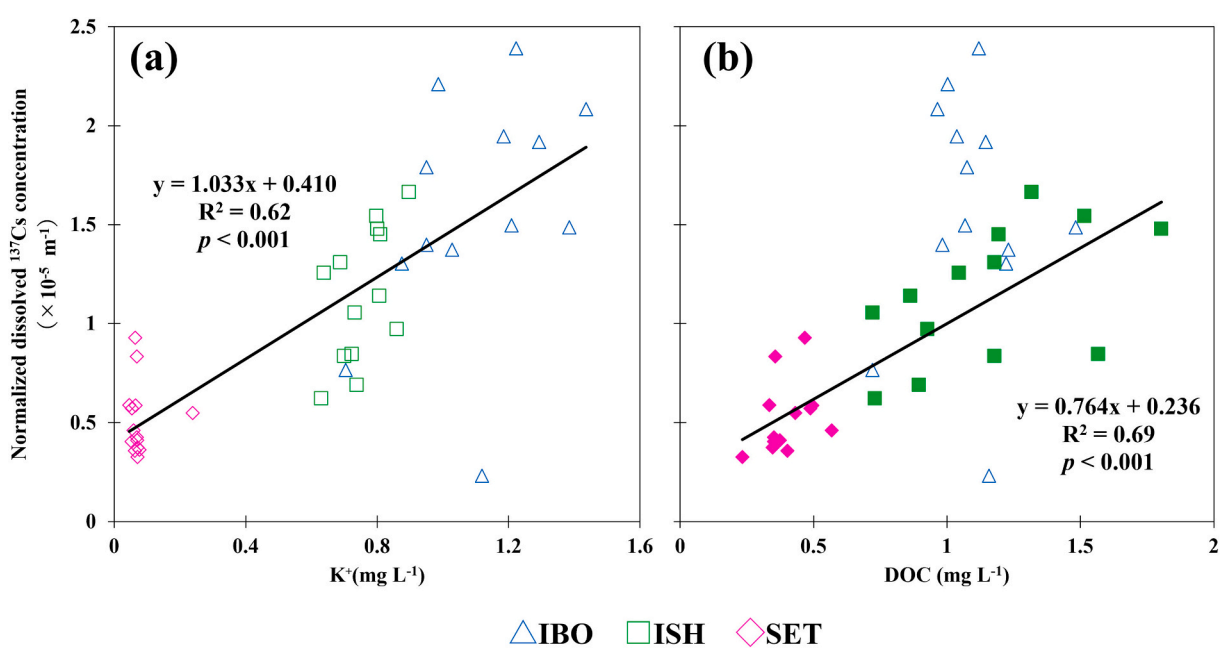

Fig. 6. Normalized Diss ^{137}Cs concentrations in three catchments (IBO, ISH, and SET) plotted against (a) K^+ and (b) DOC concentrations. The correlation equation between Normalized Diss ^{137}Cs concentrations and DOC was calculated by two catchments (ISH and SET; closed marker) with smaller K^+ concentration.

no significant trend was observed for ISH and SET. A significant positive correlation between DOC and the water temperature was observed only for SET ($R^2 = 0.62$, $p = 0.0024$), and no significant trend was observed for IBO and ISH. From these figures, the IBO, which has many tributaries in its headwaters, and the SET, which is in its headwaters, show quite different water quality characteristics in terms of water temperature dependence, and the ISH shows intermediate characteristics between them.

A number of studies have shown that (e.g., Tsuji et al., 2016) the seasonal variation in Diss ^{137}Cs concentrations is largely influenced by the contribution of K^+. However, in our study, the K^+ concentrations at SET were much lower than those reported previously. Furthermore, K^+ concentrations at SET did not change much regardless of water temperature, whereas Diss ^{137}Cs concentrations showed a clear seasonal trend (Fig. 4). These results indicate that K^+ concentration is one of the factors controlling Diss ^{137}Cs concentration, as in previous studies, but that it is not the most important factor. The relationships between the normalized Diss ^{137}Cs and DOC/K^+ concentrations were investigated as shown in Fig. 6. In SET, the smallest catchments in this study, K^+ concentrations were much lower than those previously reported as K^+ concentrations associated with Diss ^{137}Cs concentrations. In IBO, K^+ concentrations were relatively high, and Diss ^{137}Cs concentrations tended to increase with increasing K^+ concentrations. On the other hand, in ISH, the increase in dissolved ^{137}Cs in response to temperature change was observed, whereas the increase in K^+ was less, and this is quite related to the increase in DOC. These results suggest that although K^+ concentration is generally one of the factors controlling Diss ^{137}Cs concentrations, the results indicate that it is not an important factor in a source head area such as SET.

Therefore, we plotted the relationship between DOC and ^{137}Cs concentrations (Fig. 6b). Although there is an overall relationship between DOC and Cs, we focus on SET and ISH, which have low K^+ concentrations, and examine the correlation between DOC and ^{137}Cs concentrations. The correlation between DOC and ^{137}Cs concentration is good ($R^2 = 0.69$, $p < 0.001$). These results indicate that K^+ is undoubtedly an important factor controlling the ^{137}Cs concentration in the system effluent, but at the head of the watershed where the concentration of K^+ is low, a relationship with DOC is observed. These results suggest that the K^+ concentration is one of the factors controlling the Diss ^{137}Cs concentration, as in previous studies, but DOC also would be a significant factor in headwater streams such as SET.

4. Discussion

Igarashi et al. (2022) investigated seasonal variations in the concentration of Diss ^{137}Cs in the middle reaches of the Abukuma River and reported that peaks appeared in May (spring) and July (summer) of approximately 1.3 and 1.25 times the reference value (obtained by fitting Eq. (7)), respectively. In contrast, in this study, the concentration of Diss ^{137}Cs peaked in July or August at approximately 1.3 times the reference value. The peak occurred once a year. Igarashi et al. (2022) suggested that the peak in May was caused by an increase in K^+ concentrations in river water owing to fertilizer run-off associated with the annual soil puddling of agricultural land in May. The absence of a peak in May in this study, which did not include agricultural land in the catchment, supports the contribution of K^+ to the seasonal variation in Diss ^{137}Cs concentrations owing to agricultural activities (e.g., paddling). Tsuji et al. (2016) and Hayashi et al. (2022) suggested a relationship between K^+ and Diss ^{137}Cs concentrations in rivers. However, experiments in the upper reaches of rivers (Hayashi et al., 2022) and leaching experiments using forest litter with different degrees of degradation (Kurihara et al., 2020) have shown that K^+ has a substantially higher leaching rate during the early stages of degradation of organic matter than ^{137}Cs, with a cumulative leaching rate after 120 h, which is approximately 10 times higher than that of ^{137}Cs. The rate of ^{137}Cs release due to organic matter decomposition may have been small, resulting in a smaller rate-temperature dependence. On the other hand, since Cs is more difficult to release than K^+, the effect of temperature on the decomposition rate of organic matter may have been more pronounced.

The positive correlation between normalized Diss ^{137}Cs and K^+ concentration observed in this study, similar to those in previous studies, indicates that the K^+ observed in this study is likely to be of organic rather than terrestrial agricultural activities origin (SS load and fertilizer runoff), as no agricultural land is included in the study catchment. In contrast, the peak concentrations of Diss ^{137}Cs in the summer obtained for the small headwater catchments in this study were approximately 1.5 and 2.0 times higher than those in the other seasons. In contrast, Igarashi et al. (2022), whose study included agricultural land, showed a smaller increase in Diss ^{137}Cs concentrations in summer than the present study, with peaks of approximately 1.25 times baseline in July and approximately 1.3 times baseline in May. The greater seasonal variation in Diss ^{137}Cs concentrations in the headwaters than in the river basin is consistent with several forest litter leaching experiments (Kurihara et al., 2020; Sakai et al., 2015; Sakakibara et al., 2021; Sakuma et al., 2021), supporting the hypothesis that Diss ^{137}Cs in the upper catchments originates from organic matter. Although DOC in river water can originate from a variety of sources, because the watersheds in this study are headwater streams consisting of mountain forests, forest litter is likely the main source of the majority of DOC. In temperate forests, DOC concentrations in the horizon solution vary seasonally depending on the soil temperature, which depends on microbial activities that are enhanced by temperature (Fujii et al., 2011). In addition, the temporal variation of DOC concentrations in soil water was similar to that in stream water (Kawasaki et al., 2007), and no NH_4^+ has been detected in headwater catchments. This implies that Diss ^{137}Cs leaching associated with the decomposition of Org, such as litter, by microorganisms is important in small forested catchments in headwaters. In fact, the total length of the stream channel from the spring to the sampling point is 37 m for SET and 306.8 m for ISH, whereas it is 573.2 m for IBO, as shown in Table 1. The longer channel length means that the possibility of K^+ leaching from organic matter, sediment, etc. into the stream water during the stream flow process is greater. On the other hand, at the headwaters, where the distance from the spring is very short, the organic matter decomposition in the litter is the source of Cs, and thus the correlation of DOC as an indicator of organic matter decomposition is considered better.

Future studies are needed to determine the leaching process of Diss ^{137}Cs and the contribution of Diss ^{137}Cs over time in organic-rich small headwater catchments. Continuous measurements of ^{137}Cs, K^+, and DOC concentrations at the same survey locations will provide an enhanced dataset and allow for more meaningful analyses, especially at SET, which has extremely low K^+ concentrations. It is also important to measure Diss ^{137}Cs, DOC, and K^+ concentrations in the Kuchibuto River, which is downstream of the study sites, and to compare the relationships between Diss ^{137}Cs, DOC, and K^+ concentrations with those in small headwater catchments. Also, studies on the adsorption/desorption of ^{137}Cs and chemical composition of water in various headwaters in the process of flowing from spring water to stream water and river water should be conducted in many watersheds in the future.

5. Conclusion

In this study, the concentrations of Diss, CSS, and Org ^{137}Cs in the stream waters of four small headwater catchments in the Yamakiya district of Fukushima Prefecture were observed for approximately 12.0 years after the FDNPP accident. Based on these long-term observations, the elution of ^{137}Cs from SS and Org was evaluated in terms of the solid-liquid partition coefficients and the relationship between Diss ^{137}Cs, K^+, and DOC concentrations. Furthermore, the normalized CSS ^{137}Cs concentrations at IBO, where decontamination was carried out, decreased rapidly by approximately one order of magnitude during the

decontamination period and tended to maintain low concentrations thereafter. In contrast, the concentration of Diss ^{137}Cs decreased temporarily during the decontamination period; however, after decontamination, it tended to recover to post-decontamination levels. A significant seasonal variations were observed in Diss ^{137}Cs concentrations, which were highest in summer (approximately 1.5 to 2.0 times higher than the reference value) from July to August, and lowest in winter. In the SET and ISH watersheds, where water flow from the groundwater spring is short, there was a correlation between DOC concentration and dissolved ^{137}Cs concentration, while in the IBO watershed, where the distance from the groundwater spring is long, there was a temperature dependence and a good correlation between K^+ and ^{137}Cs. Therefore, microbial decomposition of organic matter may have a significant effect on the seasonal variation of dissolved ^{137}Cs in forested headwater streams at short distances from the springs, but the influence of competing ions is expected to increase gradually as the water flows downstream.

CRediT authorship contribution statement

Taichi Kawano: Conceptualization, Methodology, Validation, Investigation, Writing – original draft, Visualization. **Yuichi Onda:** Funding acquisition, Conceptualization, Investigation, Project administration, Supervision, Writing - review & editing. **Hiroaki Kato:** Supervision. **Junko Takahashi:** Supervision, Data curation, Formal analysis, Investigation, Methodology, Validation, Visualization, Writing - review & editing.

Declaration of competing interest

The authors declare the following financial interests/personal relationships which may be considered as potential competing interests: Yuichi Onda reports financial support and travel were provided by University of Tsukuba. Yuichi Onda reports a relationship with University of Tsukuba that includes: employment.

Data availability

Data will be made available on request.

Acknowledgment

We acknowledge funding support from the commission study of the Ministry of Education, Culture, Sports, Science and Technology (MEXT) FY 2011–2012, Nuclear Regulation Authority (NRA) FY 2013–2014, Japan Atomic Energy Agency-funded FY2015-2021, Grant-in-Aid for Scientific Research on Innovative Areas (grant number 24110005), Grant-in-Aid for Scientific Research (A) 22H00556, and Japan Science and Technology Agency (JST) as part of the Belmont Forum.

References

Beck, H.E., Zimmermann, N.E., McVicar, T.R., Vergopolan, N., Berg, A., Wood, E.F., 2018. Present and future köppen-geiger climate classification maps at 1-km resolution. Sci. Data 5. https://doi.org/10.1038/sdata.2018.214.

Brouwer, E., Baeyens, B., Maes, A., Cremers, A., 1983. Cesium and rubidium ion equilibria in illite clay. J. Phys. Chem. 87, 1213–1219. https://doi.org/10.1021/j100230a024.

Delvaux, B., Kruyts, N., Cremers, A., 2000. Rhizospheric mobilization of radiocesium in soils. Environ. Sci. Technol. 34, 1489–1493. https://doi.org/10.1021/es990658g.

Eyrolle-Boyer, F., Boyer, P., Garcia-Sanchez, L., Métivier, J.M., Onda, Y., de Vismes, A., Cagnat, X., Boulet, B., Cossonnet, C., 2016. Behaviour of radiocaesium in coastal rivers of the Fukushima Prefecture (Japan) during conditions of low flow and low turbidity – insight on the possible role of small particles and detrital organic compounds. J. Environ. Radioact. 151, 328–340. https://doi.org/10.1016/j.jenvrad.2015.10.028.

Fujii, K., Funakawa, S., Shinjo, H., Hayakawa, C., Mori, K., Kosaki, T., 2011. Fluxes of dissolved organic carbon and nitrogen throughout Andisol, Spodosol and Inceptisol profiles under forest in Japan. Soil Sci. Plant Nutr. 57, 855–866. https://doi.org/10.1080/00380768.2011.637304.

Funaki, H., Tsuji, H., Nakanishi, T., Yoshimura, K., Sakuma, K., Hayashi, S., 2022. Remobilisation of radiocaesium from bottom sediments to water column in reservoirs in Fukushima, Japan. Sci. Total Environ. 812, 152534 https://doi.org/10.1016/j.scitotenv.2021.152534.

Garcia-Sanchez, L., Konoplev, A.V., 2009. Watershed wash-off of atmospherically deposited radionuclides: a review of normalized entrainment. J. Environ. Radioact. 100, 774–778. https://doi.org/10.1016/j.jenvrad.2008.08.005.

Hayashi, S., Tsuji, H., Ishii, Y., 2022. Effects of forest litter on dissolved ^{137}Cs concentrations in a highly contaminated mountain river in Fukushima. J. Hydrol. Reg. Stud. 41, 101099 https://doi.org/10.1016/j.ejrh.2022.101099.

He, Q., Walling, D.E., 1996. Interpreting particle size effects in the adsorption of ^{137}Cs and unsupported ^{210}Pb by mineral soils and sediments. J. Environ. Radioact. 30, 117–137. https://doi.org/10.1016/0265-931X(96)89275-7.

IAEA, 2020. Environmental transfer of radionuclides in Japan following the accident at the Fukushima Daiichi nuclear power plant. In: IAEA TECDOC 1927.

Igarashi, Y., Nanba, K., Wada, T., Wakiyama, Y., Onda, Y., Moritaka, S., Konoplev, A., 2022. Factors controlling the dissolved ^{137}Cs seasonal fluctuations in the Abukuma River under the influence of the nuclear power plant accident. J. Geophys. Res. Bio. 127, 1–16. https://doi.org/10.1029/2021JG 006591.

Iwagami, S., Onda, Y., Tsujimura, M., Abe, Y., 2017a. Contribution of radioactive ^{137}Cs discharge by suspended sediment, coarse organic matter, and dissolved fraction from a headwater catchment in Fukushima after the Fukushima Dai-ichi Nuclear Power Plant accident.-474. J. Environ. Radioact. 166, 466–474. https://doi.org/10.1016/j.jenvrad.2016.07.025.

Iwagami, S., Tsujimura, M., Onda, Y., Nishino, M., Konuma, R., Abe, Y., Hada, M., Pun, I., Sakaguchi, A., Kondo, H., Yamamoto, M., Miyata, Y., Igarashi, Y., 2017b. Temporal changes in dissolved ^{137}Cs concentrations in groundwater and stream water in Fukushima after the Fukushima Dai-ichi Nuclear Power Plant accident. J. Environ. Radioact. 166, 458–465. https://doi.org/10.1016/j.jenvrad.2015.03.025.

Iwagami, S., Onda, Y., Sakashita, W., Tsujimura, M., Satou, Y., Konuma, R., Nishino, M., Abe, Y., 2019a. Six-year monitoring study of ^{137}Cs discharge from headwater catchments after the Fukushima Dai-ichi Nuclear Power Plant accident. J. Environ. Radioact. 210 https://doi.org/10.1016/j.jenvrad.2019. 106001.

Iwagami, S., Tsujimura, M., Onda, Y., Konuma, R., Satou, Y., Sakakibara, K., Yoschenko, V., 2019b. Dissolved ^{137}Cs concentrations in stream water and subsurface water in a forested headwater catchment after the Fukushima Dai-ichi Nuclear Power Plant accident. J Hydrol. 73, 688–696. https://doi.org/10.1016/j.jhydrol.2019.04.019.

Kalbitz, K., Solinger, S., Park, J.-H., Michalzik, B., Matzner, E., 2000. Controls on the dynamics of dissolved organic matter in soils: a review. Soil Sci. 165, 277–304.

Kato, H., Onda, Y., Gao, X., Sanada, Y., Saito, K., 2019. Reconstruction of a Fukushima accident-derived radiocesium fallout map for environmental. J. Environ. Radioact. 210, 105996 https://doi.org/10.1016/j.jenvrad.2019.105996.

Kawasaki, M., Ohte, N., Kabeya, N., Katsuyama, M., 2007. Hydrological control of dissolved organic carbon dynamics in a forested headwater catchment, Kiryu Experimental Watershed, Japan. Hydrol. Process. 22, 429–442. https://doi.org/10.1002/hyp.6615.

Konoplev, A.V., Bulgakov, A.A., Popov, V.E., Hilton, J., Coman, R., N, J., 1996. Long-Term Investigation of ^{137}Cs Fixation. Soils Radiat. Prot. Dosim. 64, 15–18. https://doi.org/10.1093/oxfordjournals.rpd.a031555.

Konoplev, A., Golosov, V., Laptev, G., Nanba, K., Onda, Y., Takase, T., Wakiyama, Y., Yoshimura, K., 2016. Behavior of accidentally released radiocesium in a soil-water environment: looking at Fukushima from a Chernobyl perspective. J. Environ. Radioact. 151, 568–578. https://doi.org/10.1016/j.jenvrad.2015.06.019.

Konopleva, I., Klemt, E., Konoplev, A., Zibold, G., 2009. Migration and bioavailability of ^{137}Cs in forest soil of southern Germany. J. Environ. Radioact. 100, 315–321. https://doi.org/10.1016/j.jenvrad.2008.12.010.

Kurihara, M., Onda, Y., Yasutaka, T., 2020. Differences in leaching characteristics of dissolved radiocaesium and potassium from the litter layer of Japanese cedar and broadleaf forests in Fukushima, Japan. J. Environ. Radioact. 223-224 https://doi.org/10.1016/j.jenvrad.2020.106417.

Liu, C., Zachara, J.M., Qafoku, O., Smith, S.C., 2003. Effect of temperature on Cs^+ sorption and desorption in subsurface sediments at the Hanford Site, U.S.A. Environ. Sci. Technol. 37, 2640–2645. https://doi.org/10.1021/es026221h.

Matsuzaki, S., Tanaka, A., Kohzu, A., Suzuki, K., Komatsu, K., Shinohara, R., Nakagawa, M., Nohara, S., Ueno, R., Satake, K., Hayashi, S., 2021. Seasonal dynamics of the activities of dissolved ^{137}Cs and the ^{137}Cs of fish in a shallow, hypereutrophic lake: links to bottom-water oxygen concentrations. Sci. Total Environ. 761, 143257 https://doi.org/10.1016/j.scitotenv.2020.143257.

McKinley, J.P., Zachara, J.M., Heald, S.M., Dohnalkova, A., Newville, M.G., Sutton, S.R., 2004. Microscale distribution of cesium sorbed to biotite. Environ. Sci. Technol. 38, 1017–1023. https://doi.org/10.1021/es034569m.

Meentemeyer, V., 1978. Macroclimate the lignin control of litter decomposition rates. Ecology 59, 465–472. https://doi.org/10.2307/1936576.

Ministry of Environment, 2015. FY2014 Decontamination Report - A Complication of experiences to date on decontamination for the living environment Conducted by Ministry of Environment, p. 422.

Monte, L., 1997. A collective model for predicting the long-term behaviour of radionuclides in rivers. Sci. Total Environ. 201, 17–19. https://doi.org/10.1016/S0048-9697(97)84049-1.

Nakanishi, T., Sakuma, K., 2019. Trend of ^{137}Cs concentration in river water in the medium term and future following the Fukushima nuclear accident. Chemosphere 215, 272–279. https://doi.org/10.1016/j.chemosphere.2018.10.017.

Nakanishi, T., Matsunaga, T., Koarashi, J., Atarashi-Andoh, M., 2014. ^{137}Cs vertical migration in a deciduous forest soil following the Fukushima Dai-ichi Nuclear Power

Plant accident. J. Environ. Radioact. 128, 9–14. https://doi.org/10.1016/j.jenvrad.2013.10.019.

Nakanishi, T., Funaki, H., Sakuma, K., 2021. Factors affecting ^{137}Cs concentrations in river water under base-flow conditions near the Fukushima Dai-ichi. J. Radioanal. Nucl. Chem. 328, 1243–1251. https://doi.org/10.1007/s10967-021-07735-7.

Nakao, A., Thiry, Y., Funakawa, S., Kosaki, T., 2008. Characterization of the frayed edge site of micaceous minerals in soil clays influenced by different pedogenetic conditions in Japan and northern Thailand. Soil Sci. Plant Nutr. 54, 479–489. https://doi.org/10.1111/j.1747-0765.2008.00262.x.

Naulier, M., Eyrolle-Boyer, F., Boyer, P., Métivier, J.M., Onda, Y., 2017. Particulate organic matter in rivers of Fukushima: an unexpected carrier phase for radiocesiums. Sci. Total Environ. 579, 1560–1571. https://doi.org/10.1016/j.scitotenv.2016.11.165.

Ochiai, S., Ueda, S., Hasegawa, H., Kakiuchi, H., Akata, N., Ohtsuka, Y., Hisamatsu, S., 2016. Spatial and temporal changes of ^{137}Cs concentrations derived from nuclear power plant accident in river waters in eastern Fukushima, Japan during 2012-2014. J. Radioanal. Nucl. Chem. 307, 2167–2172. https://doi.org/10.1007/s10967-015-4442-5.

Onda, Y., Taniguchi, K., Yoshimura, K., Kato, H., Takahashi, J., Wakiyama, Y., Coppin, F., Smith, H., 2020. Radionuclides from the Fukushima Daiichi Nuclear Power Plant in terrestrial systems. Nat. Rev. Earth Environ. https://doi.org/10.1038/s43017-020-009-x.

Peel, M.C., Finlayson, B.L., Mcmahon, T.A., 2007. Updated World Map of the Köppen-Geiger Climate Classification Hydrology and Earth System Sciences Updated World Map of the Köppen-Geiger Climate Classification. Hydrol. Earth Syst. Sci. 11, 1633–1644. https://doi.org/10.5194/hess-11-1633-2007.

Phillips, J.M., Russell, M.A., Walling, D.E., 2000. Time-integrated sampling of fluvial suspended sediment: a simple methodology for small catchments. Hydrol. Process. 14, 2589–2602. https://doi.org/10.1002/1099-1085(20001015)14:14<2589::AID-HYP94>3.0.CO;2-D.

Rosén, K., 1996. Transfer of radiocaesium in sensitive agricultural environments after the Chernobyl fallout in Sweden. Sci. Total Environ. 182, 135–145. https://doi.org/10.1016/0048-9697(95)05059-0.

Sakai, M., Gomi, T., Naito, R.S., Negishi, J.N., Sasaki, M., Toda, H., Nunokawa, M., Murase, K., 2015. Radiocesium leaching from contaminated litter inforest streams. J. Environ. Radioact. 144, 15–20. https://doi.org/10.1016/j.jenvrad.2015.03.001.

Sakakibara, K., Iwagami, S., Tsujimura, M., Konuma, R., Sato, Y., Onda, Y., 2021. Radiocesium leaching from litter during rainstorms in the Fukushima broadleaf forest. Sci. Total Environ. 796. https://doi.org/10.1016/j.scitotenv.2021.148929.

Sakuma, K., Yoshimura, K., Nakanishi, T., 2021. Leaching characteristics of ^{137}Cs for forest floor affected by the Fukushima nuclear accident: A litterbag experiment. Chemosphere 264, 128480. https://doi.org/10.1016/j.chemosphere.2020.128480.

Salamanca, E.F., Kaneko, N., Katagiri, S., 2003. Rainfall manipulation effects on litter decomposition and the microbial biomass of the forest floor. Appl. Soil Ecology. 22, 271–281. https://doi.org/10.1016/S0929-1393(02)00153-1.

Sawhney, B.L., 1972. Selective sorption and fixation of cations by clay minerals: a review. Clay Clay Miner. 20, 93–100.

Smith, J.T., Cross, M.A., Wright, S.M., 2002. Predicting transfers of ^{137}Cs in terrestrialand aquatic environments: A whole-ecosystem approach. Radioprot. Collolues 37, 37–42. https://doi.org/10.1051/radiopro/2002071.

Smith, J.T., Wright, S.M., Cross, M.A., Monte, L., Kudelsky, A.v., Saxén, R., Vakulovsky, S.M., Timms, D.N., 2004. Global analysis of the riverine transport of ^{90}Sr and ^{137}Cs. Environ. Sci. Technol. 38, 850–857. https://doi.org/10.1021/es0300463.

Takahashi, J., Hihara, D., Sasaki, T., Onda, Y., 2022. Evaluation of contribution rate of the infiltrated water collected using zero-tension lysimeter. Sci. Total Environ. 816, 151983 https://doi.org/10.1016/j. scitotenv.2021.151983.

Taniguchi, K., Onda, Y., Smith, H.G., Blake, W., Yoshimura, K., Yamashiki, Y., Kuramoto, T., Saito, K., 2019. Transport and redistribution of radiocesium in fukushima fallout through Rivers. Environ. Sci. Technol. 53, 12339–12347. https://doi.org/10.1021/acs.est.9b02890.

Tegen, I., Dorr, H., 1996. Mobilization of cesium in organic rich soils: correlation with production of dissolved organic carbon. Water Air Soil Pollut. 88, 133–144.

Tertre, E., Berger, G., Castet, S., Loubet, M., Giffaut, E., 2005. Experimental sorption of Ni^{2+}, Cs^{+} and Ln^{3+} onto a montmorillonite up to 150°C. Geochim. Cosmochim. Acta 69, 4937–4948. https://doi.org/10.1016/j.gca.2005.04.024.

Tsuji, H., Nishikiori, T., Yasutaka, T., Watanabe, M., Ito, S., Hayashi, S., 2016. Behavior of dissolved radiocesium in river water in a forested watershed in Fukushima Prefecture. J. Geophys. Res. Biogeosci. 121, 2588–2599. https://doi.org/10.1002/2016JG003428.

Tsuji, H., Funaki, H., Watanabe, M., Hayashi, S., 2022. Effects of temperature and oxygen on ^{137}Cs desorption from bottom sediment of a dam lake. Appl. Geochem. 140, 105333 https://doi.org/10.1016/j.apgeochem.2022.105303.

Wada, T., Konoplev, A., Wakiyama, Y., Watanabe, K., Furuta, Y., Morishita, D., Kawata, G., Nanba, K., 2019. Strong contrast of cesium radioactivity between marine and freshwater fish in Fukushima. J. Environ. Radioact. 204, 132–142. https://doi.org/10.1016/j.jenvrad.2019.04.006.

Wauters, J., Elsen, A., Cremers, A., Konoplev, A.V., Bulgakov, A.A., Comans, R.N.J., 1996. Prediction of solid/liquid distribution coefficients of radiocesium in soils and sediments. Part one: a simplified procedure for the solid phase characterization. Appl. Geochem. 11, 589–594. https://doi.org/10.1016/0883-2927(96)00027-3.

Yoshimura, K., Onda, Y., Kato, H., 2015. Evaluation of radiocaesium wash-off by soil erosion from various land uses using USLE plots. J. Environ. Radioact. 139, 362–369. https://doi.org/10.1016/j.jenvrad.2014.07.019.